



Contents lists available at ScienceDirect

Journal of Traditional and Complementary Medicine

journal homepage: www.elsevier.com/locate/jtcme

Electroacupuncture improves articular microcirculation and attenuates cartilage hypoxia in a male rabbit model of knee osteoarthritis

Ma Weiwei^a, Du Mei^a, Lu Juan^b, Xing Longfei^a, Chen Xilin^a, Hu Tingyao^a, Zhu Wenting^a, Guo Changqing^{a,*}

^a School of Acupuncture, Moxibustion and Tuina, Beijing University of Chinese Medicine, Beijing, PR China

^b Shenzhen Hospital of Southern Medical University, Shenzhen, PR China

ARTICLE INFO

JEL classification:
the experimental approach

Keywords:
Electroacupuncture
Osteoarthritis
Cartilage
GLUT1
PKM2
LDHA
Microcirculation
Rabbit

ABSTRACT

Background and aim: Hypoxia of the cartilage has been considered as a potential pathogenic factor in knee osteoarthritis (KOA). Studies have shown that impaired blood perfusion of joint leads to cartilage hypoxia. Electroacupuncture (EA) has proven effects on pain relief and improving microcirculation. This study aimed to explore the effect of EA on articular microcirculation and cartilage anoxic and the underlying mechanisms.

Procedures: Videman's method was used for 6 weeks to establish the KOA model. EA intervention was performed in four points around the knee for 3 weeks after KOA modeling. The Lequesne MG score was used to assess ethology. We recorded the oxygen tension of synovial fluid and the synovial microcirculation in vivo. HE-staining was used to assess cartilage morphology, and immunohistochemistry (IHC), Western blotting, and RT-PCR were used to assess expression of the major glycolytic enzymes glucosetransporter1 (GLUT1), pyruvate kinase M2 (PKM2), and lactate dehydrogenase A (LDHA). Enzyme-linked immunosorbent assay (Elisa) was used to detect lactate content.

Results and conclusion: There was a significant decrease in Lequesne MG score and improvement in Mankin score after EA intervention ($P < 0.01$), a significant increase in synovial microcirculation ($P < 0.05$) and synovial fluid oxygen tension ($P < 0.01$), and there was significant decrease in the expression of GLUT1, PKM2 and LDHA ($P < 0.01$) and lactate ($P < 0.05$). This study suggested that EA ameliorate cartilage hypoxia and regulate glycolytic metabolism in chondrocytes in KOA model rabbits by improving articular microcirculation and oxygen tension.

1. Introduction

Knee osteoarthritis (KOA) is characterized by synovial inflammation, cartilage degeneration and subchondral bone sclerosis, but the main pathological feature is articular cartilage degeneration. KOA is a major public health problem affecting 500 million people worldwide,¹ with the elderly being disproportionately affected by the condition.² The main cause of KOA in older adults is movement disorders and disabilities, which place a significant burden on individuals and society. The treatments for KOA are mainly pharmacotherapy, physiotherapy, and rehabilitation in the early stage. Electroacupuncture (EA) is a relatively common therapy in Chinese medicine that has reached the clinical effect

of KOA,^{3,4} but its mechanism needs further investigation.

Tissue oxygen supply is mainly controlled by the distribution of blood vessels.⁵ Cartilage is an avascular tissue that exists in a hypoxic environment⁶ and receives its oxygen and nutrients from the superficial synovial blood vessels.^{7,8} The plasma in the synovial capillaries is filtered to form synovial fluid and secreted into the joint lumen, which carries oxygen and nutrients.⁹ The oxygen partial pressure (PO₂) of synovial fluid in healthy joints is 3–11 kPa, which may reflect the oxygen homeostasis of the joint cavity.¹⁰ Hypoxia, a condition caused by low PO₂, is a relevant feature of osteoarthritis affecting angiogenesis, inflammation, apoptosis, cartilage degradation and energy metabolism.¹¹ Abnormal activation of tissue hypoxia-induced transcriptional

Abbreviations: EA, Electroacupuncture; KOA, Knee Osteoarthritis; OARSI, Osteoarthritis Research Society International; ELISA, Enzyme-linked immunosorbent assay; IHC, Immunohistochemical; WB, Western Blot; GLUT1, Glucosetransporter1; PKM2, Pyruvate Kinase M2; LDHA, Lactate dehydrogenase A; PO₂, Oxygen Partial Pressure; BP, Blood perfusion; BV, Blood velocity.

* Corresponding author. School of Acupuncture, Moxibustion and Tuina, Beijing University of Chinese Medicine, No. 11 East North Third Ring Road, Chaoyang District, Beijing, 100029, PR China.

E-mail address: 603060@bucm.edu.cn (G. Changqing).

<https://doi.org/10.1016/j.jtcme.2024.01.002>

Received 1 June 2023; Received in revised form 8 December 2023; Accepted 5 January 2024

Available online 6 January 2024

2225-4110/© 2024 Center for Food and Biomolecules, National Taiwan University. Production and hosting by Elsevier Taiwan LLC. This is an open access article under the CC BY-NC-ND license (<http://creativecommons.org/licenses/by-nc-nd/4.0/>).

pathways may contribute to metabolic changes and result in cartilage lesions.¹² Under low oxygen tension, HIF-1 α upregulates the expression of metabolic enzymes, transporters, and mitochondrial proteins involved in glucose metabolism and redirects energy metabolism from oxidative phosphorylation to glycolysis.¹³ As KOA progresses, increased intraarticular pressure can decrease synovial blood flow due to vascular susceptibility to mechanical load, which inhibits the diffusion and transfer of oxygen from synovial capillaries into synovial fluid,¹⁴ and the PO₂ decreases to 1–1.25 kPa and further contributes to cartilage hypoxia. Therefore, the improvement of the synovial microcirculation and the synovial fluid PO₂ in the joint cavity is the target of the remedy of cartilage hypoxia.

The guidelines for non-surgical KOA treatment issued by Osteoarthritis Research Society International (OARSI) recommend that biomechanical intervention for KOA treatment is applicable in different populations.¹⁵ EA is a non-surgical treatment that acts on the muscles and combines traditional acupuncture with electrical stimulation to reduce pain and improve functional activity, recommended under the American College of Rheumatology guidelines on KOA.¹⁶ The electrical stimulation effect of EA on acupoints has unique properties in alleviating pain and movement disorders that have achieved continuous therapeutic effects.^{17,18} Studies have shown that EA is effective in chondrocyte apoptosis and collagen synthesis, preventing cartilage degradation and delaying the pathological progression of KOA.^{19,20} According to genetic analysis, EA induces similar changes as movement in skeletal muscles, partially activates similar signaling pathways that induce glucose uptake and improve metabolic disorders.^{21–23} EA intervention can attenuate pain via regulation of expression of multiple proteins in the hypothalamus, while there was a significant regulation of glycolysis metabolism pathway.²⁴ Studies showed that EA can activate AMP-activated protein kinase (AMP-APK) and enhance the process of glycolysis in the early stage of Alzheimer's disease, the expression of proteins associated with glycolysis in the hippocampus was increased, including pyruvate kinase M2 (PKM2).²⁵ EA can effectively upregulate GLUT1 expression in the hippocampus in cerebral ischemia rats by raising the glucose transportation of microvascular endothelial cells.²⁶

Therefore, this study investigated the effect of EA on synovial microcirculation and synovial fluid PO₂, the glycolytic pathway in the chondrocytes, lactate and the key enzymes associated with chondrocytes hypoxia to explore whether EA could improve articular microcirculation, synovial fluid PO₂, and the hypoxic state of the joint cavity.

2. Materials and methods

2.1. Animals

A total of 18 purebred male New Zealand rabbits, weighing 2.5 kg, were purchased from Beijing Fulong Tengfei Experimental Animal Research Institute Ltd. (Certificate Number: SYXK 2018–0041). The rabbits were acclimated to the environment for one week and had free access to food and water. The animals were reared under the appropriate conditions at a temperature of 18–20 °C and a relative humidity of 40%–60%. This experiment has been approved by the Beijing University of Chinese Medicine Committee on Ethics of Animal Experiments (Approval Number: BUCM-4-2,022,041,502-2114). The procedure was performed strictly according to the Guidance Suggestions for the Care and Use of Laboratory Animals (2021) by the Ministry of Science and Technology of China.²⁷

^a Peer review under responsibility of The Center for Food and Biomolecules, National Taiwan University.

Table 1
Standard of Lequesne MG scores.

| Items | Behavioral manifestation of animals | Scores |
|--|--|--------|
| Local pain reaction through palpation | No abnormal pain response. | 0 |
| | Mild contraction of affected hind limb. | 1 |
| | Contraction of affected hind limb with systemic reaction, such as shaking, turning head to lick. | 2 |
| | Severe contraction of affected hind limb with shaking, struggling or escaping. | 3 |
| Gait change | Normal gait without limping. | 0 |
| | Mild limping when running. | 1 |
| | The affected hind limb could participate in walking but limped obviously. | 2 |
| | The affected hind limb couldn't participate in walking, touch or pedal the ground. | 3 |
| Passive range of motion of affected joint (Straight position = 0°) | Above 90° | 0 |
| | 45°~90° | 1 |
| | 15°~45° | 2 |
| | Below 15° | 3 |
| Degree of joint swelling | No swelling, bone markers clearly visible. | 0 |
| | Mild swelling, bone markers shallow. | 1 |
| | Obvious swelling, disappearance of bone markers. | 2 |

2.2. Induction of KOA models

Eighteen New Zealand rabbits were randomized into three groups: control group (n = 6), model group (n = 6), and EA group (n = 6). Videman's method was used for 6 weeks to induce the KOA model.²⁸ The rabbits were fasted and dehydrated for 16 h. Then they were anesthetized through the ear vein by intravenous injection of 3% pentobarbital sodium solution (30 mg/kg). After complete anesthesia, rabbits were placed on the operating table. Their left hindlimb was wrapped with pressure-sensitive adhesive tape, double-sided foam tape and resin bandages from groin to ankle, fixed the knee in a straight position.²⁹ Finally, a splint was used in the outer layer to prevent the rabbits from biting. Blood circulation and swelling of the toes were observed daily during the modeling weeks. After 6 weeks of immobilization, the bandages were removed and adjusted for 3 days. Animals in control group were grasped daily during KOA modeling and intervention period.

2.3. EA intervention

After removing the bandages in the EA group, four main acupoints in the left hindlimb were selected: Liangqiu (ST34), Xuehai (SP10), Waixiyan (ST35) and Neixiyan (EX-LE4). After disinfection, needle was inserted into each acupoint and connected to electrode clips of the Han's Acupoint Nerve Stimulator (LH202H, Beijing Huawei Industry Development Company, China) (frequency: 2/100 Hz, intensity: 2 mA, 20 min).³⁰ EA intervention was performed on EA group once every other day for 3 weeks.³¹

2.4. Ethological assessment

After the bandages were removed, the modified Lequesne MG Arthritis Level Rating Scale for pain and motility was assessed in each group to evaluate model.³² The items were scored according to the scale. The results of the Lequesne MG scores from model rabbits were >1, which indicated that all KOA modeling was successful. The rabbit's passive range of motion was measured with goniometer, the axis of it was opposed to the lateral femoral condyle, parallel to the long axis of the femur, and the axis of motion was parallel to the long axis of the tibia when the knee joint of KOA's left hind limb was passively flexed. And the flexion angle value was read when the knee joint was flexed to the minimum amplitude. After 3 weeks of intervention, Lequesne MG score was evaluated again on each group. The details of Lequesne MG Arthritis

Level Rating Scale presented in [Table 1](#).

2.5. Detection of synovial fluid oxygen pressure and microcirculation in vivo

2.5.1. Synovial fluid oxygen partial pressure

The rabbits were anesthetized with 3 % pentobarbital sodium solution (30 mg/kg), placed in the supine position, the temperature was maintained at 37 °C by a heating pad, and the ambient temperature was kept constant at 28 °C. The depth of anesthesia was determined by response to noxious stimuli applied to the ear. The skin of left knee joint was exposed and the underlying fascia was removed on either side of the patella. To avoid damage to the oxygen partial pressure probe, the probe was inserted into the articular cavity in a 10 mL syringe-needle from the lateral side of the patellar ligament into the articular cavity and connected to a Microx TX3 instrument (Microx TX3, Regensburg, Germany). Images were recorded continuously for 90 s and the measurements were analyzed with the customized TX3v602 software.

2.5.2. Synovial microcirculation

The synovial microcirculation was recorded with a laser Doppler perfusion instrument (Moor Instruments, Millwey, Axm, UK). The underlying fascia was exposed of the left knee joint through longitudinal incisions on either side of the patella. Three synovial regions of interest (ROI) were selected: the suprapatellar sac, the anterior cruciate ligament, and the subpatellar fat pad. A laser needle probe was inserted into the suprapatellar bursa, fixed on adjustable height stands and connected to the instrument. Images of a continuous length of 90 s were recorded and measurements analyzed using moorVMS customized PC software. The ROI was selected on the area of the synovial in the joint: (1) the suprapatellar sac, the largest synovial sac in the knee which communicates with the joint cavity; (2) The anterior cruciate ligament, which surrounded by the synovial membrane; (3) The subpatellar fat pad, adipose tissue between the synovial membrane and the fibrous layer of the joint capsule. The synovial membrane covers the subpatellar fat pad and extends posteriorly toward the intercondylar fossa.

2.6. HE staining of the cartilage

Cartilage sections were sequentially treated with dimethylbenzene for dewaxing and an ethanol decreasing gradient for hydration. Sections were stained with hematoxylin for 5 min and rinsed with distilled water. After treatment with 1 % hydrochloric acid-ethanol solution for 3 s, the sections were transferred to eosin for 3 min and then covered with neutral balsa for observation and analysis of changes in chondrocyte morphology and cartilage thickness with Mankin score.³³

2.7. Immunohistochemistry (IHC)

Paraffin-embedded cartilage slices (4 µm) were obtained and baked for 30 min at 65 °C, deparaffinized in xylene and rehydrated in alcohol and deionized water. Then the cells were incubated with 0.3 % hydrogen peroxidase. Incubation with primary antibodies was performed after blocking the sections with 10 % normal goat serum (Abcam) for 30 min Against GLUT1 (Proteintech, 1:200), PKM2 (Bioss, 1:200), and LDHA (Proteintech, 1:100) overnight at 4 °C. The secondary antibody used was biotinylated antirabbit IgG conjugated to HRP (1:200, Servicebio, Wuhan, China). The chromogenic reaction appeared after incubating with DAB for 28 s. The staining was then visualized and photographed in 5 different fields using an optical microscope.

2.8. Western blot analysis

After the cartilage was completely ground, total proteins were extracted using RIPA lysis buffer, centrifuged at 12,000 rpm for 20 min at 4 °C, the supernatant collected. BCA protein assay kits (Pierce

Table 2

Primers used in this study.

| Gene | Primer sequences |
|-------|--|
| GLUT1 | Forward: GAGCGTCATCTTCGTCCA Reverse: CCAGGATGGTGACCTTCTTCTC |
| PKM2 | Forward: CCTCCAGTCACTCCACAGACCT Reverse: CTGCCAGACTCCGTCAGAACTA |
| LDHA | Forward: GTTAGGCACCGATGACAGACAA Reverse: ATGCACCTCTGAGATTCTTC |
| GAPDH | Forward: TTCAGTATGATTCCACCCACG Reverse: GGGCTGAGATGATGACCCCTTT |

Biotechnology) were used to determine total protein concentration. Polyacrylamide gel electrophoresis was used to separate the proteins, which were then transferred to PVDF membranes and blocked with 5 % non-fat milk for 2 h, and the samples were incubated with primary antibodies overnight at 4 °C. The following primary antibodies were used: GLUT1 (Proteintech, 1:1000), PKM2 (Bioss, 1:1000), and LDHA (Proteintech, 1:2000). β-Actin (Proteintech, 1:2000) was used as an internal reference. Secondary antibody (HRP-labeled goat anti-rabbit 1:10,000, Servicebio, Wuhan, China) was incubated for 1 h at room temperature. Electrochemiluminescence (Servicebio, Wuhan, China) reagent was applied to the membranes in a darkroom, and images were acquired with a ChemiDoc XRS+ (Bio-Rad Laboratories, Hercules, CA, USA). Image-Pro Plus software 5.0 was used to analyze the grayscale value of the protein bands. The target protein to β-actin was used to calculate the relative protein concentrations of GLUT1, PKM2 and LDHA.

2.9. Real-time PCR

Total RNA was extracted from cartilage using TRIzol reagent (Servicebio, Beijing, China) and transcribed into cDNA using RT First Strand cDNA Synthesis Kit (Servicebio, Beijing, China) according to the instructions. The cDNA amplification was analyzed in triplicate by real-time PCR (RT-PCR) using 2 × SYBR Green PCR Master Mix (Servicebio, Beijing, China). The expression of the genes was calculated using the $2^{-\Delta\Delta Ct}$ method. The primer sequences are shown in [Table 2](#).

2.10. ELISA of lactate

ELISA kits were used for concentration determination and relative calculation of lactate according to the instructions. Briefly, blank control, standard and sample wells were processed, and 50 µl of the samples were loaded with biotinylated binding protein on target-coated plastic plates and into monoclonal antibody-coated 96-well plates and incubated for 2 h at room temperature. After washed with washing buffer, the plates were incubated with detection antibodies. Then the immunoreactivity of the sample was measured by adding the substrate solution, incubating in the dark for 30 min at room temperature and then adding the stop solution. Finally, the absorbance was recorded by a multiscan approach (MK3, Thermo, USA) at a wavelength of 450 nm to obtain optical density (OD) values. The lactate content of the cartilage was determined using the standard curves of the linear regression calculation.

2.11. Statistical analysis

Statistical analysis was performed using IBM SPSS 20.0 software. All experimental results were expressed as mean ± standard deviation (SD). All datasets were tested for normality and homogeneity of variance. One-way ANOVA with the Least Significant Difference (LSD) test was used for comparisons of between-group differences when variance and normal test conditions were met. When homogeneity of variance or normality failed, the Kruskal-Wallis independent-samples test was used. Differences were considered statistically significant at $P < 0.05$ and $P < 0.01$.

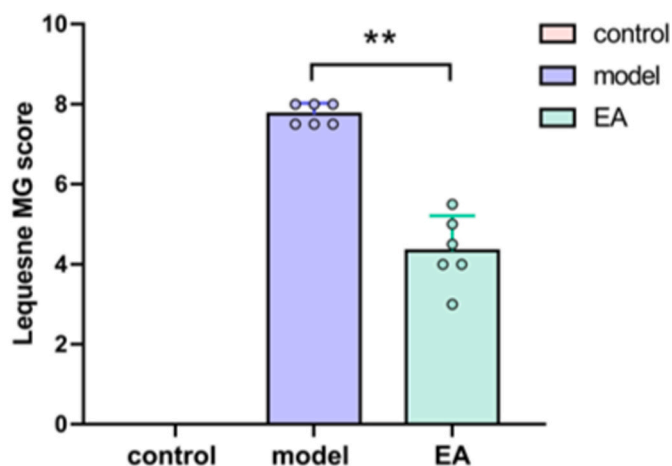


Fig. 1. The evaluation of Lequesne MG scores after EA intervention. $**P < 0.01$ vs. KOA group.

3. Results

3.1. EA improved ethology in KOA rabbits

We used Lequesne MG scores to assess ethology in KOA rabbits. Results showed that Lequesne MG score was significantly increased in the model group compared to the control group ($P < 0.01$). After an intervention period of 3 weeks, Lequesne MG score was significantly decreased in the EA group compared to those in the model group ($P < 0.01$) (Fig. 1). These results indicated that EA intervention could improve ethology in KOA rabbits.

3.2. EA restored cartilage degeneration by improving the morphological disorder and increasing cartilage thickness in KOA

The main pathologic feature of KOA is cartilage degeneration. HE staining was used to observe the pathological changes in the cartilage tissue and to assess the extent of cartilage degeneration (Fig. 2A). HE staining of the cartilage showed no defect of the cartilage surface and disorganized chondrocytes in the control group. The structure of the cartilage was clear, the cells at all levels were neatly and regularly arranged, and the shape was normal. In the model group, chondrocytes manifested as aggregation, cracks, and a coarse and disordered arrangement. The tidal line was blurred and angiogenesis was observed in the subchondral bone. In the EA group, the cartilage surface was smooth without cracks, the cells were neatly arranged in a columnar array, repeated tidal lines and some chondrocyte defects were seen, the cell morphology was normal, and there was a small amount of subchondral bone angiogenesis. The Mankin score was used to analyze HE-stained histological sections (Fig. 2C).

Partial-thickness and full-thickness defects are relevant for the development of cartilage damage in KOA (Fig. 2B). Compared to the control group, the TAC was significantly decreased in the KOA group ($P < 0.01$). Compared to the model group, the TAC was significantly increased in the EA group ($P < 0.01$) (Fig. 2D). The intervention effect of EA group was observed from the perspective of morphology, in which the pathological manifestations and Mankin score showed that EA effectively reduced cartilage Mankin score and restored cartilage morphology and thickness to reverse KOA cartilage degeneration.

3.3. EA improved synovial microcirculation and synovial fluid oxygen tension in KOA

The synovial microcirculation was monitored using laser Doppler to reflect changes in blood flow in the joint cavity. The oxygen partial pressure of synovial fluid measured by the oxygen partial pressure

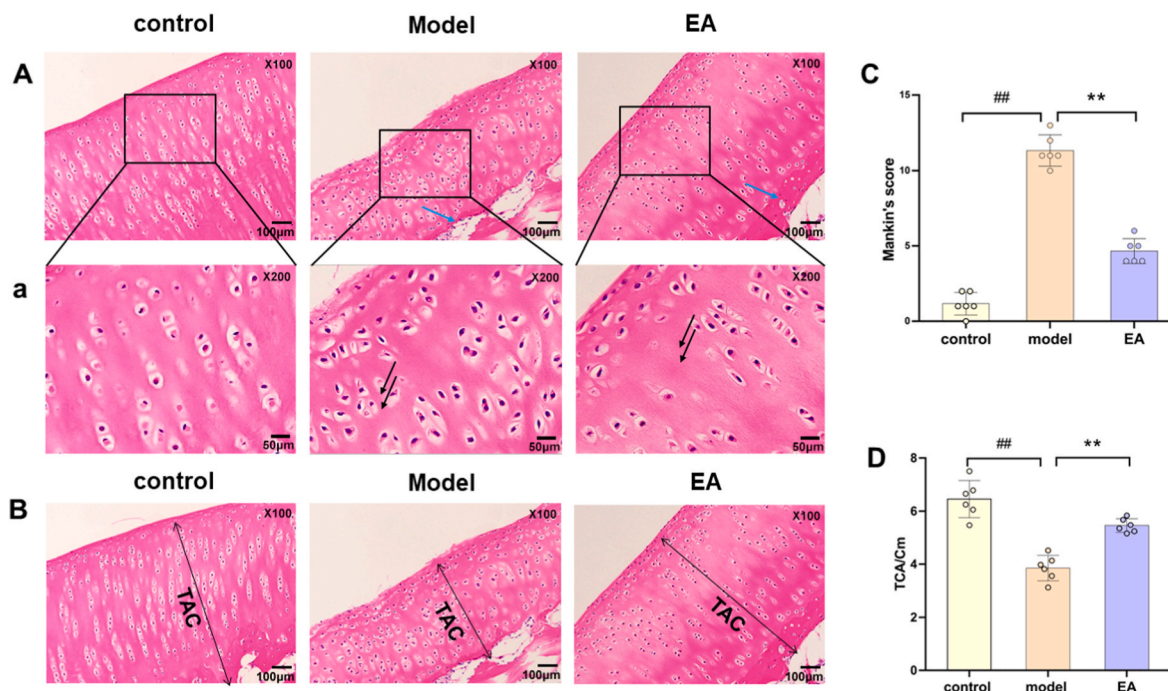


Fig. 2. Effect of EA on the histological morphology of the articular cartilage and the thickness of the cartilage layer. (A) The images show typical pathological changes in each cartilage group stained with HE. a: partial magnification (Black arrow: cell aggregation/deficiency; Blue arrow: angiogenesis; scale bar = 50 μ m, magnification 200). (B) Histology stained with HE of the cartilage showed the thickness of the cartilage in three groups (scale bar = 100 μ m, magnification 100). (C) Mankin score evaluation. Values are presented as SEM means and scatterplot. $##P < 0.01$ vs. control group, $**P < 0.01$ vs. KOA group. (D) Analysis of cartilage layer thickness. $##P < 0.01$ vs. control group, $**P < 0.01$ vs. KOA group.

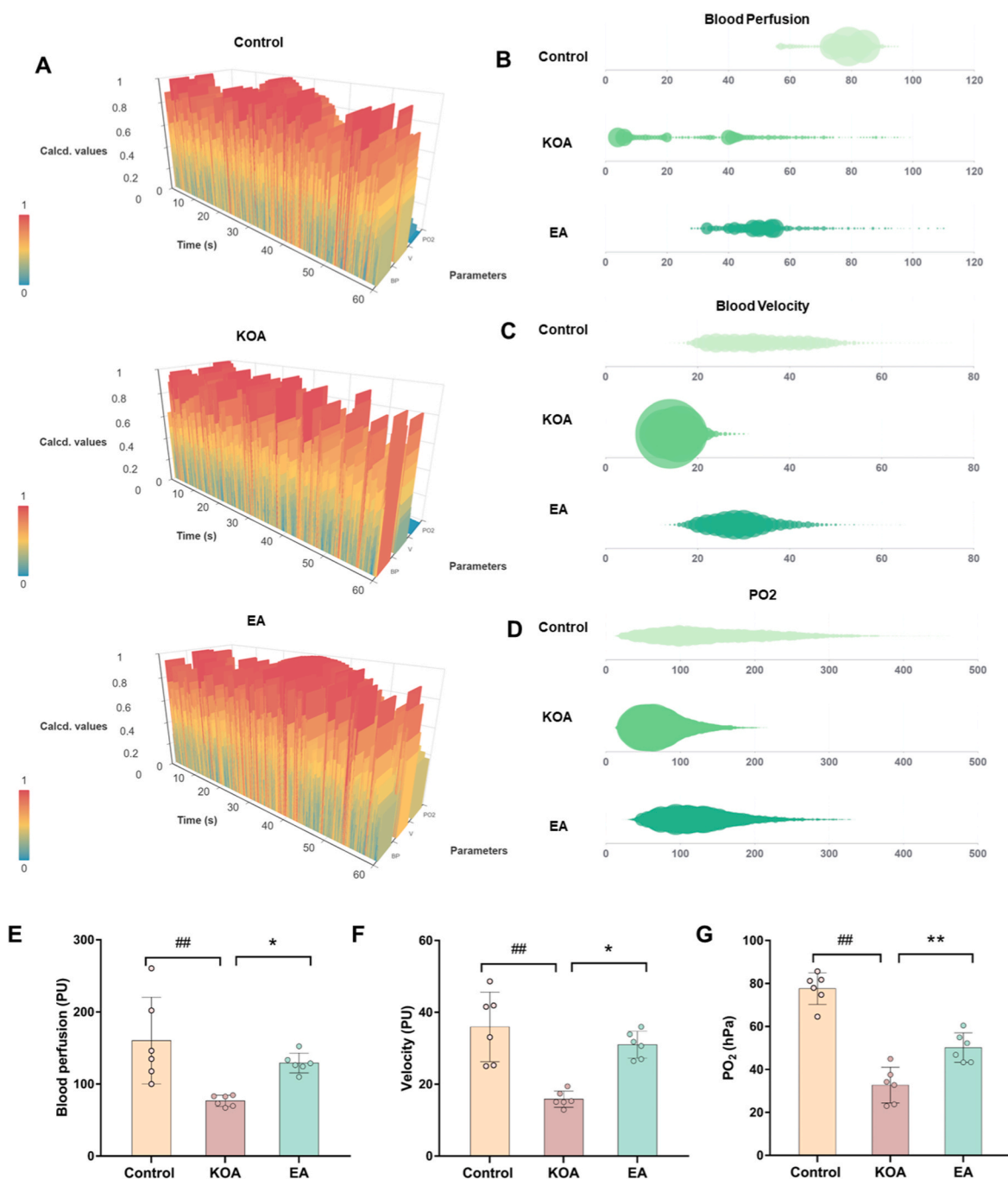


Fig. 3. Effect of EA on synovial microcirculation and partial pressure of oxygen in synovial fluid. (A) Dynamic distribution of synovial microcirculation and PO₂ in each group. (B–D) Distribution section of BP, BV and PO₂ in each group. (E–G) The distribution and values of the BP, BV and synovial fluid PO₂ were compared. ##P < 0.01 vs. control group, **P < 0.01 vs. KOA group, *P < 0.05 vs. KOA group.

monitor reflected the oxygen environment in the joint cavity. The 3-D cylindrical module reflected the dynamic changes of synovial microcirculation blood perfusion (BP), blood velocity (BV) and synovial fluid PO₂ in Fig. 3A. Compared with the control group (10–400 PU), the distribution of BP in the KOA group (10–200 PU) was lower. EA intervention increased the data distribution area (40–300 PU) (Fig. 3B). Compared with the control group (20–60 PU), the distribution area of BV in the KOA group was lower (8–30 PU), and EA intervention could improve the data distribution area (16–60 PU) (Fig. 3C). Synovial microcirculation in the model group decreased significantly compared to the control group, including BP (P < 0.01) and BV (P < 0.01).

However, the synovial microcirculation in the EA group increased significantly compared to that in the model group in terms of BP (P < 0.05) and BV (P < 0.05) (Fig. 3E/F).

In the control group, PO₂ data were mainly distributed in the 56–96 hPa interval, and concentrated in the 72–90 hPa interval. In contrast, PO₂ in KOA group was lower (2–100 hPa), and the distribution was discrete. After EA intervention, the distribution interval of PO₂ increased (32–58 hPa) (Fig. 3D). PO₂ of synovial fluid results showed that PO₂ was significantly reduced in the model group compared to the control group (P < 0.01) and significantly reduced in the EA group (P < 0.01) compared to model group rise (Fig. 3G). These results suggested that EA

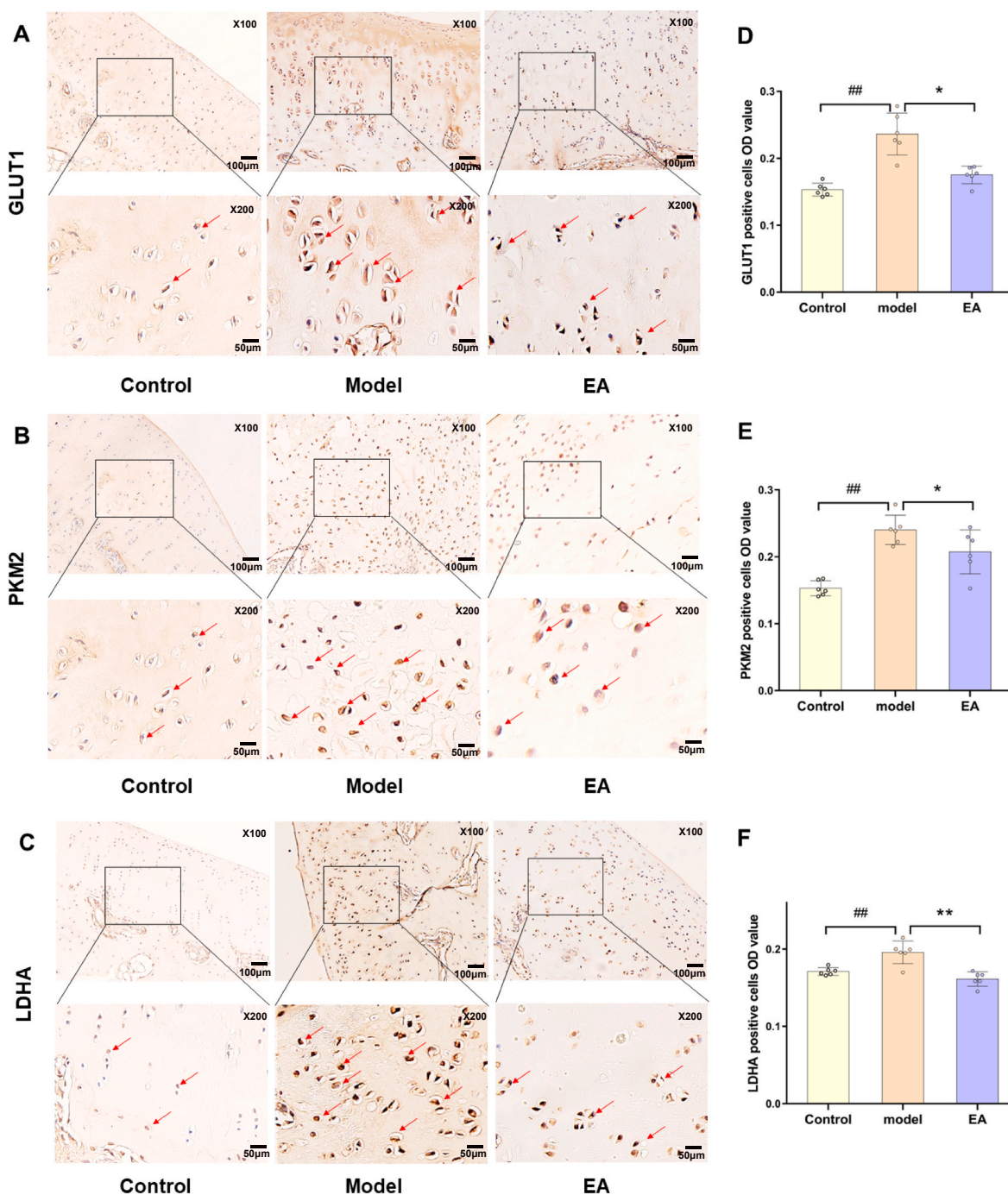


Fig. 4. IHC assessment of GLUT1, PKM2 and LDHA expression in articular cartilage. (A–C) Representative images of IHC staining for GLUT1, PKM2 and LDHA in cartilage sections of the four groups. Scale bar = 100 μm, Magnification 100. Scale bar = 50 μm, partial magnification 200. (D–F) Semi-quantitative analysis of GLUT1, PKM2 and LDHA positive areas in the articular cartilage of the three groups. ##P < 0.01 vs. control group, **P < 0.01 vs. KOA group, *P < 0.05 vs. KOA group.

improve the hypoxic state of the joint cavity by increasing synovial microcirculation and PO₂ of synovial fluid in the joint cavity of the KOA rabbits.

3.4. EA downregulated the expression of key enzymes involved in glycolysis under hypoxic conditions in KOA cartilage

To assess the changes in oxygen content and glycolytic metabolism in chondrocytes, we detected the expression of the major glycolytic enzymes GLUT1, PKM2 and LDHA in chondrocytes by IHC, Western blot and RT-PCR.

IHC showed that GLUT1, PKM2 and LDHA were all expressed in the nucleus and cytoplasm as shown in Fig. 4A–C. Compared to the control group, the OD value results showed that the positive cell expression of GLUT1, PKM2 and LDHA was significantly increased in the model group (P < 0.01; P < 0.01; P < 0.01). Data were significantly reduced in the EA group compared to the model group (P < 0.05; P < 0.05; P < 0.01) (Fig. 4D–F).

Western blot analysis of GLUT1, PKM2 and LDHA showed similar results. Representative bands of major glycolytic enzyme expression in cartilage were shown in Fig. 5A. Compared to the control group, the results of the WB assay showed that the protein expression of GLUT1,

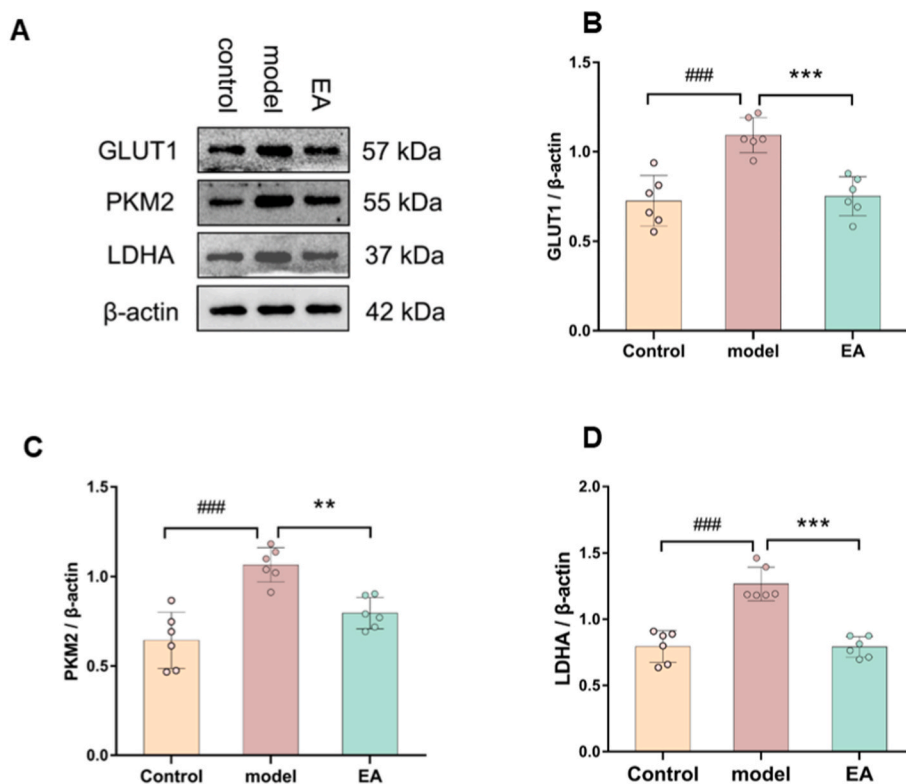


Fig. 5. The effect of EA on the relative protein expression of GLUT1, PKM2, and LDHA in KOA cartilage was tested by the density of bands as fold changes after normalization to β -actin. **(A)** The bands of expression of key glycolytic enzymes in the three groups. **(B–D)** Ratios of GLUT1/ β -actin, PKM2/ β -actin and LDHA/ β -actin measured by Western blot. ### $P < 0.01$ vs. the control group, # $P < 0.05$ vs. control group. ** $P < 0.01$ vs. KOA group, * $P < 0.05$ vs. KOA group.

PKM2 and LDHA was significantly increased in the model group ($P < 0.01$; $P < 0.01$; $P < 0.05$). However, they were all significantly reduced in the EA group compared to the model group ($P < 0.01$; $P < 0.01$; $P < 0.05$) (Fig. 5B–D).

PCR analysis of GLUT1, PKM2 and LDHA further confirmed the results (Fig. 6A–C). Compared to the control group, the results of the PCR assay showed that the relative mRNA expression of GLUT1, PKM2 and LDHA in the model group were all significantly increased ($P < 0.01$; $P < 0.01$; $P < 0.01$). The three proteins were all decreased in the EA group compared to the model group ($P < 0.05$; $P < 0.05$; $P < 0.05$). These results demonstrated that the effect of EA on the regulation of oxygen levels and glycolytic metabolism can be exerted by suppressing the expression of GLUT1, PKM2 and LDHA in the chondrocytes of KOA rabbits.

3.5. EA reduced the lactate content of the glycolysis products in the KOA cartilage

We analyzed the lactate content of glycolytic metabolism production in the three groups. The results showed that the articular cartilage lactate content was lower in the control group than in the model group ($P < 0.01$). However, it was significantly reduced in the EA group compared to the model group ($P < 0.05$) (Fig. 6D). These results indicated that EA intervention could reduce lactate accumulation in KOA cartilage.

4. Discussion

This study aimed to determine the efficacy of EA in regulating articular microcirculation and cartilage oxygen levels in the joint cavity. The results of this study showed that the Videman method induced

cartilage hypoxia in KOA via decreased synovial microcirculation and synovial fluid PO_2 and accelerated glycolysis metabolism of chondrocytes, which in turn induced degeneration of articular cartilage. EA restored the cartilage degeneration which was observed from the structural morphology and thickness of the cartilage by HE staining. EA could improve synovial microcirculation and synovial fluid PO_2 and slow down the rate of glycolysis, which was manifested as the decreased levels of the major glycolytic enzymes GLUT1, PKM2 and LDHA and lactate in the cartilage tissue of KOA rabbits. Therefore, EA intervention ameliorated cartilage hypoxia and regulated glycolytic metabolism in chondrocytes in KOA model rabbits by improving articular microcirculation and PO_2 .

The synovial membrane that plays an important role in maintaining the physiological function of the joints.³⁴ Researchers adapted synovial microcirculation in assessing blood flow in the joint capsule.^{35,36} The synovial microcirculation consists of microvessels, such as arterioles, postcapillary venules, and capillaries that are involved in maintaining synovial fluid secretion and oxygen and nutrient exchange in the joint cavity to maintain homeostasis of the synovial environment.³⁷ Cartilage is nourished by oxygen provided by the synovial fluid.³⁸ Abnormal hemodynamics, insufficient oxygen supply and release of inflammatory factors caused by abnormal synovial microcirculatory structure and dysfunction are the common pathologic mechanisms of osteoarthritis.^{39–41} Studies have shown that the intra-articular pressure in KOA increases significantly and far exceeds the end-perfusion pressure of the synovial capillaries, resulting in blocked blood flow of the synovial capillaries, and hypoperfusion causes the oxygen partial pressure of the synovial fluid to decrease.⁴² Studies also found that increased intra-articular pressure restricted synovial blood flow, which could be the reason for the lower PO_2 in KOA joints.⁴³ Clinical experiments have shown that oxygen tension in the synovial fluid from normal joints

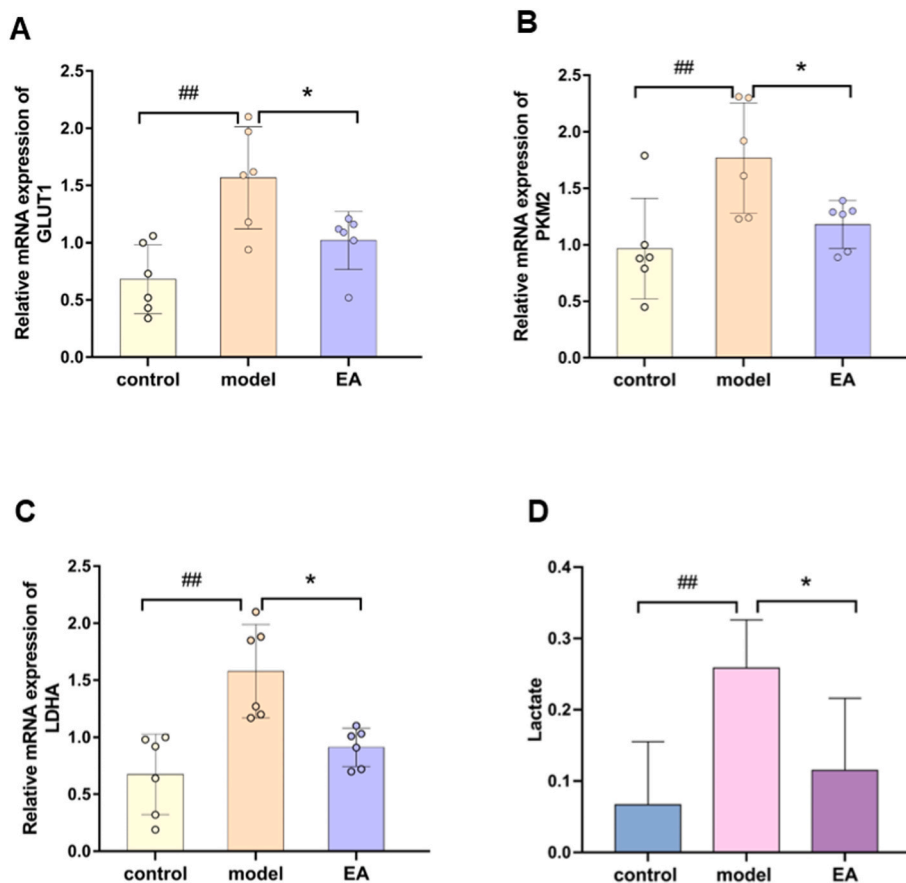


Fig. 6. Effect of EA on the expression of GLUT1, PKM2 and LDHA was measured by RT-PCR and lactate content by Elisa in KOA cartilage. (A–C) Real-time PCR analysis of GLUT1, PKM2 and LDHA in the three groups. ##P < 0.01 vs. control group, *P < 0.05 vs. KOA group. (D) Effect of EA on the lactate content of KOA cartilage. ##P < 0.01 vs. control group, *P < 0.05 vs. KOA group.

ranges from 50 to 60 mmHg and varies from 20 to 71 mmHg in patients with osteoarthritis.⁴⁴ Sustained hypoperfusion reduced oxygen tension and resulted in a reduction in oxygen compulsion from the synovial fluid. Further reduction in cartilage oxygen uptake from synovial fluid eventually leads to hypoxia of KOA chondrocytes. Therefore, blockage of synovial microcirculation may reduce synovial fluid partial pressure of oxygen and further aggravate knee joint hypoxia. In this study, we found that synovial microcirculation of KOA rabbits was blocked, synovial blood flow and blood velocity were significantly decreased, and this change was accompanied by a decrease in synovial fluid partial pressure of oxygen. After 3 weeks of EA intervention, synovial blood flow and blood velocity were improved compared to those in the KOA group. Similar results were found for the oxygen partial pressure of the synovial fluid. The results of the present study demonstrated that joint immobilization in rabbits resulted in a reduction in joint capsule blood flow and PO₂, and EA interventions could improve joint microcirculation and PO₂ and further improve joint hypoxia in KOA rabbits.

Functional maintenance of chondrocytes and synthesis of extracellular matrix of chondrocytes were mainly depend on the balance of glucose metabolism in chondrocytes.⁴⁵ *In vitro* studies have shown that chondrocyte metabolism was anaerobic at low PO₂.⁴⁶ Anaerobic metabolism produces acid that provides a pH more conducive to acidophilic degradative enzymes, allowing components of the cartilage matrix to be digested. Hypoxia alters chondrocyte bioenergetics by promoting glycolysis, which in turn induces cartilage degeneration mechanisms.⁴⁷ It is supported by study that increased glycolysis *in vitro* was reflected, with synovial expression of GAPDH, PKM2 and GLUT1 being significantly higher in patients with synovial tissue oxygen levels <20 mm

Hg.⁴⁸ In addition, it is consistent with a recent study that PKM2 induced HIF-1 α and data from hypoxic cancer cells imply that transcription of the PKM2 gene encoding pyruvate kinase M2 was activated by HIF-1 α and the switch from the oxidative to the glycolytic metabolism.⁴⁹ Based on the clinical studies, LDHA levels in synovial fluid could be of diagnostic value to identify osteoarthritis.⁵⁰ Accordingly, our results showed a variation in energy metabolism with increased lactate production and glycolysis rate, manifested as overexpression of GLUT1, PKM2 and LDHA in chondrocytes with low synovial fluid PO₂ levels in KOA model rabbit knee joints. Then EA restricted the rate of glycolysis by regulating the expression of GLUT1, PKM2 and LDHA in chondrocytes compared to the KOA group. We also found that hypoxia increased lactate accumulation in cartilage and this change was accompanied by an increase in glycolysis rate.

In traditional Chinese medicine (TCM), KOA belongs to the category of arthralgia, which is the result of the dynamic evolution and development of muscle and bone lesions.⁵¹ According to TCM theory, the joints of the limbs are the confluence of the twelve meridians. Surrounding the knee joint are three yang and three yin meridian tendons, which are the attachment points of the tendons. It functions to connect and constrain the joint and keep joint movement.⁵² Where there are muscle and tendon lesions, qi and blood will not be able to spread smoothly into the joint cavity due to blockages in the meridians and unfavorable joint movements, leading to cartilage degeneration.⁵³ From the point of view of TCM, Waixiyan (ST35) and Neixiyan (EX-LE4) are selected according to the principle of "taking pain points as acupoints"⁵⁴, Liangqiu (ST34) and Xuehai (SP10) are the meridian points of the spleen and stomach that regulate the flow of qi and blood.⁵⁵ From

an anatomical point of view, Dubi and Neixiyan acupoints are the best choice to penetrate the joint cavity, Liangqiu and Xuehai are the main acupoints to adjust the function of the quadriceps muscle.⁵⁶

EA is a non-surgical treatment that acts on the muscles and combines traditional acupuncture with electrical stimulation. A low-frequency, dense current creates a muscle contraction, which can regulate muscle function, reduce internal pressure and mechanical stimulation of tissue, increase blood supply, relieve inflammatory irritation and pain. This study suggested that EA improve ethology, regulate synovial blood flow in the joint cavity, and restore oxygen levels to knee chondrocytes, which could be a possible mechanism to treat KOA.

5. Conclusion

In conclusion, this study found that the intervention of EA might be beneficial in relieving cartilage hypoxia, increasing cartilage oxygen levels by improving synovial microcirculation and synovial fluid PO₂ in KOA model rabbits, and further decreasing anaerobic glycolytic metabolism rate and the levels of metabolites, which could play a protective role for cartilage.

Funding

This work was provided by the National Natural Science Foundation of China (No. 81900747).

Declaration of competing interest

The authors report that they have no commercial or associative interest that represents a conflict of interest in connection with the work submitted.

References

- Hunter DJ, March L, Chew M. Osteoarthritis in 2020 and beyond: a lancet commission. *Lancet*. 2020;396(10264):1711–1712.
- Xie Y, Yu Y, Wang JX, et al. Health-related quality of life and its influencing factors in Chinese with knee osteoarthritis. *Qual Life Res*. 2020;29(9):2395–2402.
- Kelly RB, Willis J. Acupuncture for pain. *Am Fam Physician*. 2019;100(2):89–96.
- Huang H, Liang Y, Han D, et al. Case report: electroacupuncture for acute pain flare-up of knee osteoarthritis. *Front Neurol*. 2022;13, 1026441.
- Nakazawa MS, Keith B, Simon MC. Oxygen availability and metabolic adaptations. *Nat Rev Cancer*. 2016;16(10):663–673.
- Sharma L. Osteoarthritis of the knee. *N Engl J Med*. 2021;384(1):51–59.
- Findlay DM. Vascular pathology and osteoarthritis. *Rheumatology*. 2007;46(12):1763–1768.
- Blake DR, Merry P, Unsworth J, et al. Hypoxic-reperfusion injury in the inflamed human joint. *Lancet*. 1989;1(8633):289–293.
- Martel-Pelletier J, Barr AJ, Cicuttini FM, et al. Osteoarthritis. *Nat Rev Dis Prim*. 2016; 2, 16072.
- Geborek P, Lindoff B, Valind SO. Measurement of oxygen and carbon dioxide partial pressures in synovial fluid after tonometry. *Clin Physiol*. 1988;8(4):427–432.
- Warbrick I, Rabkin SW. Hypoxia-inducible factor 1- α (HIF-1 α) as a factor mediating the relationship between obesity and heart failure with preserved ejection fraction. *Obes Rev*. 2019;20(5):701–712.
- Zheng L, Zhang Z, Sheng P, et al. The role of metabolism in chondrocyte dysfunction and the progression of osteoarthritis. *Ageing Res Rev*. 2021;66, 101249.
- Ohashi Y, Takahashi N, Terabe K, et al. Metabolic reprogramming in chondrocytes to promote mitochondrial respiration reduces downstream features of osteoarthritis. *Sci Rep*. 2021;11(1), 15131.
- Quiñonez-Flores CM, González-Chávez SA, Pacheco-Tena C. Hypoxia and its implications in rheumatoid arthritis. *J Biomed Sci*. 2016;23(1):62.
- Bannuru RR, Osani MC, Vaysbrot EE, et al. OARSI guidelines for the non-surgical management of knee, hip, and polyarticular osteoarthritis. *Osteoarthritis Cartilage*. 2019;27(11):1578–1589.
- Hochberg MC, Altman RD, April KT, et al. American College of Rheumatology 2012 recommendations for the use of nonpharmacologic and pharmacologic therapies in osteoarthritis of the hand, hip, and knee. *Arthritis Care Res*. 2012;64(4):465–474.
- Tu JF, Yang JW, Shi GX, et al. Efficacy of intensive acupuncture versus sham acupuncture in knee osteoarthritis: a randomized controlled trial. *Arthritis Rheumatol*. 2021;73(3):448–458.
- Cai FH, Li FL, Zhang YC, et al. Research on electroacupuncture parameters for knee osteoarthritis based on data mining. *Eur J Med Res*. 2022;27(1):162.
- Zhang W, Gao Y, Guo C, et al. Effect of acupotomy versus electroacupuncture on ethology and morphology in a rabbit model of knee osteoarthritis. *J Tradit Chin Med*. 2019;39(2):229–236.
- Lin J, Wu G, Chen J, et al. Electroacupuncture inhibits sodium nitroprusside-mediated chondrocyte apoptosis through the mitochondrial pathway. *Mol Med Rep*. 2018;18(6):4922–4930.
- Huhtaniemi IT. Electroacupuncture mimics exercise in affecting gene expression of skeletal muscle. *J Clin Endocrinol Metab*. 2020;105(7):e2645–e2646.
- Benrick A, Pillon NJ, Nilsson E, et al. Electroacupuncture mimics exercise-induced changes in skeletal muscle gene expression in women with polycystic ovary syndrome. *J Clin Endocrinol Metab*. 2020;105(6):2027–2041.
- Mohammadnejad A, Li S, Duan H, et al. Network based analysis of microarray gene expression profiles in response to electroacupuncture. *J Tradit Complement Med*. 2019;10(5):471–477.
- Gao Y, Chen S, Xu Q, et al. Proteomic analysis of differential proteins related to anti-nociceptive effect of electroacupuncture in the hypothalamus following neuropathic pain in rats. *Neurochem Res*. 2013;38(7):1467–1478.
- Li J, Zhang B, Jia W, et al. Activation of adenosine monophosphate-activated protein kinase drives the aerobic glycolysis in Hippocampus for delaying cognitive decline following electroacupuncture treatment in APP/PS1 mice. *Front Cell Neurosci*. 2021; 15, 774569.
- Lu Y, Wang SJ, Song XT. Effects of electroacupuncture on glucose transporter-1 expression of hippocampal microvascular endothelial cells in rats with focal cerebral ischemia. *Zhen Ci Yan Jiu*. 2010;35(2):118–123.
- The Ministry of Science and Technology of the People's Republic of China. *Guidance Suggestions for the Care and Use of Laboratory Animals*. 2006.
- Videman T. Experimental osteoarthritis in the rabbit: comparison of different periods of repeated immobilization. *Acta Orthop Scand*. 1982;53(3):339–347.
- Liu J, Lin QX, Lu LM, et al. Effects of "knot-loosing" of acupotomy on motor function and morphological changes of knee joint in knee osteoarthritis rabbits. *Zhen Ci Yan Jiu*. 2021;46(2):129–135.
- Shi X, Yu W, Wang T, et al. Electroacupuncture alleviates cartilage degradation: improvement in cartilage biomechanics via pain relief and potentiation of muscle function in a rabbit model of knee osteoarthritis. *Biomed Pharmacother*. 2020;123, 109724.
- Cai FH, Li FL, Zhang YC, et al. Research on electroacupuncture parameters for knee osteoarthritis based on data mining. *Eur J Med Res*. 2022;27(1):162.
- Lequesne MG, Maheu E. Clinical and radiological evaluation of hip, knee and hand osteoarthritis. *Ageing Clin Exp Res*. 2003;15(5):380–390.
- Van der Sluijs JA, Geesink RG, van der Linden AJ, et al. The reliability of the Mankin score for osteoarthritis. *J Orthop Res*. 1992;10(1):58–61.
- Hügler T, Geurts J. What drives osteoarthritis?—synovial versus subchondral bone pathology. *Rheumatology*. 2017;56(9):1461–1471.
- Lockhart JC, Ferrell WR, Angerson WJ. Laser Doppler perfusion imaging of synovial tissues using red and near infra-red lasers. *Int J Microcirc Clin Exp*. 1997;17(3): 130–137.
- Zysk SP, Gebhard H, Plitz W, et al. Influence of orthopedic particulate biomaterials on inflammation and synovial microcirculation in the murine knee joint. *J Biomed Mater Res B Appl Biomater*. 2004;71(1):108–115.
- Levick JR. Microvascular architecture and exchange in synovial joints. *Microcirculation*. 1995;2(3):217–233.
- Svalastoga E, Kiaer T. Oxygen consumption, diffusing capacity and blood flow of the synovial membrane in osteoarthritic rabbit knee joints. *Acta Vet Scand*. 1989;30(2): 121–125.
- Paulus AC, Ebinger K, Cheng X, et al. Local biological reactions and pseudotumor-like tissue formation in relation to metal wear in a murine in vivo model. *BioMed Res Int*. 2019;2019, 3649838.
- Hartmann P, Butt E, Fehér Á, et al. Electroporation-enhanced transdermal diclofenac sodium delivery into the knee joint in a rat model of acute arthritis. *Drug Des Dev Ther*. 2018;12:1917–1930.
- Fearon U, Canavan M, Biniecka M, et al. Hypoxia, mitochondrial dysfunction and synovial invasiveness in rheumatoid arthritis. *Nat Rev Rheumatol*. 2016;12(7): 385–397.
- Rutherford DJ. Intra-articular pressures and joint mechanics: should we pay attention to effusion in knee osteoarthritis? *Med Hypotheses*. 2014;83(3):292–295.
- Wu K, Huang J, Wang Q. The use of superselective arteriography in the evaluation of the influence of intracapsular hip joint pressure on the blood flow of the femoral head. *Med Princ Pract*. 2016;25(2):123–129.
- Lund-Olesen K. Oxygen tension in synovial fluids. *Arthritis Rheum*. 1970;13(6): 769–776.
- Stegen S, Laperre K, Eelen G, et al. HIF-1 α metabolically controls collagen synthesis and modification in chondrocytes. *Nature*. 2019;565(7740):511–515.
- Tarantino R, Chiu LLY, Weber JF, et al. Effect of nutrient metabolism on cartilaginous tissue formation. *Biotechnol Bioeng*. 2021;118(10):4119–4128.
- Kierans SJ, Taylor CT. Regulation of glycolysis by the hypoxia-inducible factor (HIF): implications for cellular physiology. *J Physiol*. 2021;599(1):23–37.
- Biniecka M, Canavan M, McGarry T, et al. Dysregulated bioenergetics: a key regulator of joint inflammation. *Ann Rheum Dis*. 2016;75(12):2192–2200.
- Luo W, Hu H, Chang R, et al. Pyruvate kinase M2 is a PHD3-stimulated coactivator for hypoxia-inducible factor 1. *Cell*. 2011;145(5):732–744.
- Hurter K, Spreng D, Rytz U, et al. Measurements of C-reactive protein in serum and lactate dehydrogenase in serum and synovial fluid of patients with osteoarthritis. *Vet J*. 2005;169(2):281–285.
- Hou PW, Fu PK, Hsu HC, et al. Traditional Chinese medicine in patients with osteoarthritis of the knee. *J Tradit Complement Med*. 2015;5(4):182–196.
- Hua Z, Deng H, Tang H, et al. Clinical study of acupotomy for knee osteoarthritis based on the meridian-sinew theory: a randomized controlled clinical trial. *Evid Based Complement Alternat Med*. 2021;2021, 3987002.

53. Matos LC, Machado JP, Monteiro FJ, et al. Understanding traditional Chinese medicine therapeutics: an overview of the basics and clinical applications. *Healthcare (Basel)*. 2021;9(3):257.
54. Kaptchuk TJ. Acupuncture: theory, efficacy, and practice. *Ann Intern Med*. 2002;136(5):374–383.
55. Cai FH, Li FL, Zhang YC, et al. Research on electroacupuncture parameters for knee osteoarthritis based on data mining. *Eur J Med Res*. 2022;27(1):162.
56. Ju CJ, Zhou X, Dong CC, et al. Clinical observation of warm moxibustion therapy to improve quadriceps weakness after total knee arthroplasty. *Zhongguo Zhen Jiu*. 2019;39(3):276–279.